# The secreted protein DEL-1 activates a β3 integrin–FAK–ERK1/2–RUNX2 pathway and promotes osteogenic differentiation and bone regeneration

Received for publication, February 13, 2020, and in revised form, April 8, 2020 Published, Papers in Press, April 12, 2020, DOI 10.1074/jbc.RA120.013024

**Da-Yo Yuh[‡1], Tomoki Maekawa[‡§], Xiaofei Li[‡], Tetsuhiro Kajikawa[‡], Khalil Bdeir[¶], Triantafyllos Chavakis[‖], and George Hajishengallis[‡2]**

*From the [‡]Department of Basic and Translational Sciences, Penn Dental Medicine, University of Pennsylvania, Philadelphia, Pennsylvania 19104, the [§]Research Center for Advanced Oral Science, Graduate School of Medical and Dental Sciences, Niigata University, Niigata 951-8514, Japan, the [¶]Department of Pathology and Laboratory Medicine, Perelman School of Medicine, University of Pennsylvania, Philadelphia, Pennsylvania 19104, and the [‖]Institute for Clinical Chemistry and Laboratory Medicine, Faculty of Medicine, Technische Universität Dresden, 001069 Dresden, Germany*

Edited by Alex Toker

**The integrin-binding secreted protein developmental endothelial locus-1 (DEL-1) is involved in the regulation of both the initiation and resolution of inflammation in different diseases, including periodontitis, an oral disorder characterized by inflammatory bone loss. Here, using a mouse model of bone regeneration and *in vitro* cell-based mechanistic studies, we investigated whether and how DEL-1 can promote alveolar bone regeneration during resolution of experimental periodontitis. Compared with WT mice, mice lacking DEL-1 or expressing a DEL-1 variant with an Asp-to-Glu substitution in the RGD motif ("RGE point mutant"), which does not interact with RGD-dependent integrins, exhibited defective bone regeneration. Local administration of DEL-1 or of its N-terminal segment containing the integrin-binding RGD motif, but not of the RGE point mutant, reversed the defective bone regeneration in the DEL-1–deficient mice. Moreover, DEL-1 (but not the RGE point mutant) promoted osteogenic differentiation of MC3T3-E1 osteoprogenitor cells or of primary calvarial osteoblastic cells in a β3 integrin–dependent manner. The ability of DEL-1 to promote *in vitro* osteogenesis, indicated by induction of osteogenic genes such as the master transcription factor Runt-related transcription factor-2 (*Runx2*) and by mineralized nodule formation, depended on its capacity to induce the phosphorylation of focal adhesion kinase (FAK) and of extracellular signal-regulated kinase 1/2 (ERK1/2). We conclude that DEL-1 can activate a β3 integrin–FAK–ERK1/2–RUNX2 pathway in osteoprogenitors and promote new bone formation in mice. These findings suggest that DEL-1 may be therapeutically exploited to restore bone lost due to periodontitis and perhaps other osteolytic conditions.**

Developmental endothelial locus-1 (DEL-1)[3] is a 52-kDa protein comprising three N-terminal epidermal growth factor (EGF)-like repeats (E1–E3) followed by two C-terminal discoidin I-like domains (C1 and C2), hence also known as EGF-like repeats and discoidin I-like domains 3 (EDIL3) (1). It is secreted from distinct tissue-resident cells (*e.g.* endothelial cells, mesenchymal stem cells, osteolineage cells, and certain macrophage subsets) and associates with the cell surface or the extracellular matrix (2–6). DEL-1 interacts with different integrins, such as αvβ3 and β2 integrins (lymphocyte function-associated antigen-1 (LFA-1) and macrophage antigen-1 (Mac-1)), as well as with phospholipids, and these interactions underlie the reported biological activities of DEL-1 (1, 4, 7–10). Our group has shown that DEL-1 regulates both the initiation and resolution of inflammation (4, 5, 8, 11–14). Specifically, via the ability of endothelial cell-secreted DEL-1 to bind the LFA-1 integrin on neutrophils, DEL-1 suppresses the LFA-1–dependent firm adhesion of neutrophils to vascular endothelial cells and thereby restrains neutrophil recruitment to peripheral tissues (4, 8, 13). Moreover, the capacity of macrophage-derived DEL-1 to bridge apoptotic cells to macrophages enhances the clearance of apoptotic cells (efferocytosis) and promotes macrophage reprogramming toward a pro-resolving phenotype (4). In this regard, DEL-1 uses an RGD motif in its E2 repeat to engage the efferocytic receptor αvβ3 integrin on macrophages and its discoidin I-like domains to bind phosphatidylserine, a major "eat-me" signal on the apoptotic cell surface (4, 7). Furthermore, we have shown that the

This work was supported by National Institutes of Health Grants DE024716 (to G. H.) and DE028561 and DE026152 (to G. H. and T. C.), the University of Pennsylvania Institute for Translational Medicine and Therapeutics (ITMAT) Transdisciplinary Program in Translational Medicine and Therapeutics (to K. B.), and German Research Foundation Grant SFB1181 (to T. C.). The authors declare that they have no conflicts of interest with the contents of this article. The content is solely the responsibility of the authors and does not necessarily represent the official views of the National Institutes of Health.

[1] Present address: Dept. of Periodontology, School of Dentistry, National Defense Medical Center, Taipei 11490, Taiwan.

[2] To whom correspondence should be addressed. E-mail: geoh@upenn.edu.

[3] The abbreviations used are: DEL-1, developmental endothelial locus-1; ABC, alveolar bone crest; *Bglap*, bone γ-carboxyglutamic acid–containing protein; CEJ, cement-enamel junction; *Del1*$^{KO}$, DEL-1–deficient; EDIL3, epidermal growth factor-like repeats and discoidin I–like domain 3; ERK1/2, extracellular signal-regulated kinase 1/2; FAK, focal adhesion kinase; GAPDH, glyceraldehyde-3-phosphate dehydrogenase; ITGB3, integrin β-3; LIP, ligature-induced periodontitis; LFA-1, lymphocyte function-associated antigen-1; Mac-1, macrophage antigen-1; *Runx2*, Runt-related transcription factor-2; EGF, epidermal growth factor; KO, knockout; FAK, focal adhesion kinase; sgRNA, single guide RNA; crRNA, CRISPR RNA; MEK, mitogen-activated protein kinase/extracellular signal-regulated kinase kinase; FBS, fetal bovine serum; α-MEM, α-minimum essential medium; qPCR, quantitative real-time PCR; HRP, horseradish peroxidase; ANOVA, analysis of variance.

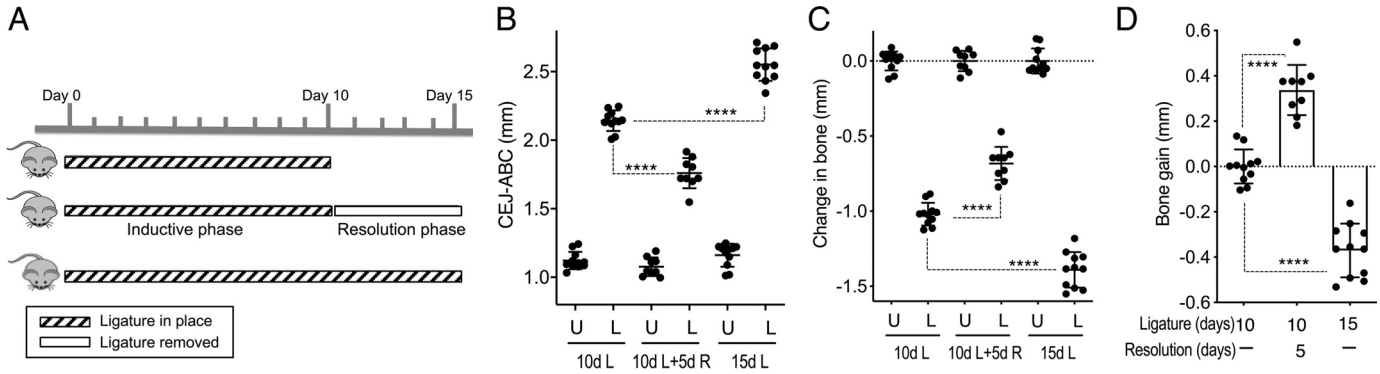


**Figure 1. Bone gain during periodontitis resolution.** *A*, outline of the model used. *B*, measurement of bone heights (distance from CEJ to ABC) in groups of WT C57BL/6 mice (8–10 weeks old) after 10 or 15 days of ligature (10d L or 15d L) or after 10 days ligature followed by 5 days without ligatures to enable resolution (10d L + 5d R). *C*, data from *B* were transformed to show bone loss in ligated (*L*) sites *versus* unligated (*U*) contralateral sites. *D*, data from *C* were transformed to show bone gain (or loss; negative values) relative to the 10d L group (baseline). Data are means ± S.D. (*error bars*) ($n = 9$–11 mice/group; pooled from two independent experiments). ****, $p < 0.0001$ (one-way ANOVA and Dunnett's post-test).

interaction of DEL-1 with the Mac-1 integrin on osteoclast precursors up-regulates the transcriptional repressor B cell lymphoma-6, which in turn inhibits the expression of the transcription factor nuclear factor of activated T cells-1 and osteoclast differentiation (14).

The importance of these homeostatic functions of DEL-1 becomes phenotypically evident in DEL-1–deficient ($Del1^{KO}$) mice in the setting of periodontitis, a prevalent inflammatory disease that affects the integrity of the tissues that surround and support the dentition, such as the gingiva and the underlying alveolar bone (15, 16). Indeed, $Del1^{KO}$ mice are highly susceptible to periodontitis featuring heavy neutrophil infiltration and interleukin-17–dependent bone loss (13). Moreover, resolution of periodontal inflammation fails in $Del1^{KO}$ mice even when the pathogenic challenge is removed (4). Specifically, in a model of ligature-induced periodontitis where bone loss is driven by the ligature-associated dysbiotic microbiome (17, 18), ligature removal promotes inflammation resolution in WT mice but not in littermate $Del1^{KO}$ mice (4).

Because inflammation resolution is a prerequisite for wound healing and regeneration of bone and other tissues (19, 20), we reasoned that DEL-1 may promote bone regeneration during periodontitis resolution. To test this hypothesis, we first established a model of alveolar bone regeneration in WT mice. Bone regeneration in this model was defective in mice lacking DEL-1 or in mice expressing a point mutant of DEL-1 that is incapable of binding the $\alpha v\beta 3$ integrin, owing to Glu-for-Asp substitution in the RGD motif of the E2 repeat. Consistent with these *in vivo* findings and with the fact that RGD-dependent interactions between the extracellular matrix and integrins regulate osteogenesis (21–24), DEL-1 could directly induce osteogenic differentiation of osteoprogenitor cells (MC3T3-E1 cells or primary calvarial osteoblastic cells) in a manner dependent on its RGD motif and on $\beta 3$ integrin expression in osteoprogenitors. Pharmacological inhibition of focal adhesion kinase (FAK) and of extracellular signal-regulated kinase 1/2 (ERK1/2) blocked the ability of DEL-1 to promote the expression of Runt-related transcription factor 2 (*Runx2*), the master osteogenic transcription factor (25, 26), and to induce mineralized nodule formation. Importantly, DEL-1, or its N-terminal segment containing the E1–E3 repeats, could restore bone regeneration in $Del1^{KO}$ mice. The ability of DEL-1 to induce new bone formation in otherwise nonhealing mice suggests that DEL-1 may be exploited therapeutically to regenerate bone for the treatment of periodontitis and perhaps other bone loss disorders.

## Results

### *Model to study bone regeneration during periodontitis resolution*

The ligature-induced periodontitis (LIP) model is used extensively to study induction of bone loss in different animal species (14, 18, 27–32). In mice, the LIP model involves the placement of a silk ligature around the maxillary second molar, while keeping the contralateral tooth unligated as baseline control (17, 18). Ligature placement simulates human periodontitis as it generates a subgingival biofilm-retentive milieu leading to dysbiotic inflammation and bone loss in conventional (but not germ-free) animals (14, 17, 18, 27–34). Ligature removal abrogates the dysbiotic microbial challenge that drives inflammatory tissue destruction and leads to disease resolution (4, 35). To study bone tissue repair in the resolving phase of periodontitis, groups of WT C57BL/6 mice were subjected to LIP with or without ligature removal. One group was euthanized after 10 days of continuous presence of ligatures (10d L). Two groups were euthanized at day 15; in one group, the ligatures were removed at day 10 to allow 5 days of resolution (10d L + 5d R), whereas in the other group the ligatures were kept until day 15 (15d L) (Fig. 1, *A–D*). Ligature removal at day 10 resulted in bone gain 5 days later in the "10d L + 5d R" group, whereas the continuous presence of ligatures in the "15d L" group caused further bone loss as compared with the "10d L" baseline (Fig. 1*D*). The bone gain in the "10d L + 5d R" group represented the formation of new bone as shown by staining coronal sections with modified Masson's trichrome, which stains mature (old) bone blue and immature (new) bone red (Fig. 2). Indeed, new (*red*) bone was detected in WT mice 5 days after ligature removal (Fig. 2, *left*), whereas essentially only old ("blue") bone was detected in similarly treated DEL-1–deficient ($Del1^{KO}$) mice, which additionally exhibited deep periodontal pocket

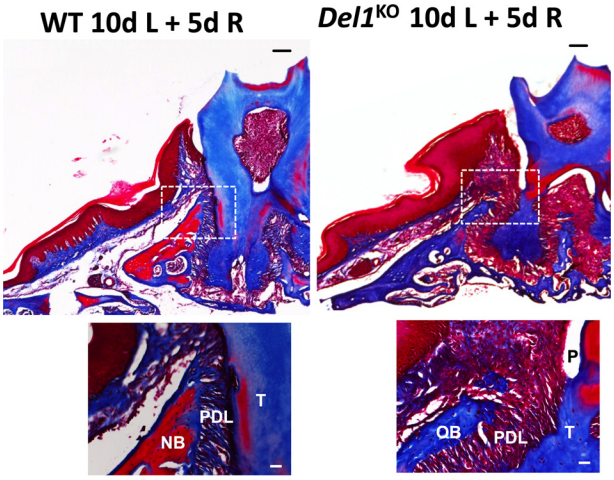


**Figure 2. Del1$^{KO}$ mice fail to generate new bone.** *Del1*$^{KO}$ mice and WT littermates were subjected to LIP for 10 days followed by 5 days without ligatures to enable resolution. Coronal sections were stained with modified Masson's trichrome, which stains old bone *blue* and new bone *red*. Shown are representative images (*scale bars*, 100 $\mu$m) and insets (*scale bars*, 25 $\mu$m) from resolution sites. *NB*, new bone; *OB*, old bone; *PDL*, periodontal ligament; *P*, pocket; *T*, tooth.

(Fig. 2, *right*). These data establish a mouse model to study bone regeneration in the resolution phase of periodontitis and suggest that endogenous DEL-1 might contribute to formation of new bone.

### *DEL-1 promotes bone gain in vivo during resolution of periodontitis*

We next examined directly the role of DEL-1 and its structural features in bone regeneration. Using the quantitative model outlined above (Fig. 1), we showed that *Del1*$^{KO}$ mice failed to gain bone during resolution (Fig. 3; results shown directly as bone gain as in Fig. 1*D*), consistent with the histological observations (Fig. 2). However, when locally injected with DEL-1-Fc or DEL-1[E1–3]-Fc, *Del1*$^{KO}$ mice gained at least as much bone as untreated WT did (Fig. 3). In contrast, *Del1*$^{KO}$ mice failed to regenerate bone when treated with Fc protein control or with DEL-1[RGE]-Fc (Fig. 3), a point mutant that does not interact with RGD-dependent integrins (such as the $\alpha v\beta 3$ integrin) due to Glu-for-Asp substitution in the RGD motif of DEL-1 (4, 5, 14). These data suggested that the N-terminal EGF-like repeats (E1–E3) of DEL-1 are sufficient to promote bone gain in *Del1*$^{KO}$ mice and the fact that the RGD motif in the E2 repeat of DEL-1 is critical for this function.

To rigorously strengthen this notion using an independent approach, we used *Del1*$^{RGE/RGE}$ mice, which were engineered to express the RGE point mutant of DEL-1. *Del1*$^{RGE/RGE}$ mice were compared with WT and *Del1*$^{KO}$ mice for their bone regeneration capacity during resolution of experimental periodontitis. We found that bone regeneration in *Del1*$^{RGE/RGE}$ mice was significantly less than seen in WT mice but was comparable with that seen in *Del1*$^{KO}$ mice (Fig. 4). Therefore, *Del1*$^{RGE/RGE}$ mice reproduced the defective phenotype of *Del1*$^{KO}$ mice in bone regeneration (Fig. 4). These data establish unequivocally that the integrin-binding RGD motif of DEL-1 is absolutely required for its ability to promote *in vivo* bone regeneration.

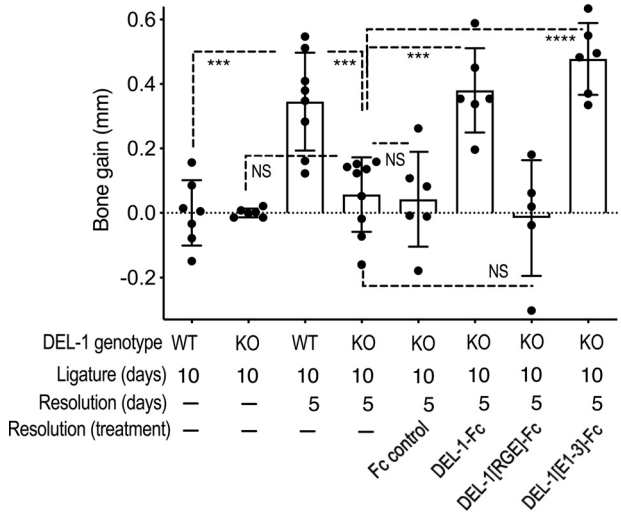


**Figure 3. DEL-1 promotes bone gain during resolution.** *Del1*$^{KO}$ mice and WT littermates (8–10 weeks old) were subjected to LIP for 10 days followed (or not) by 5 days of resolution, with or without local injection with DEL-1-Fc (1 $\mu$g) or equal molar amounts of Fc control or mutants. Treatments were performed daily (days 10–14) in *Del1*$^{KO}$ mice. Bone heights were measured, and CEJ-ABC data were transformed to indicate bone gain as outlined in Fig. 1. Data are means ± S.D. (*error bars*) ($n$ = 5–9 mice/group). ***, $p < 0.001$; ****, $p < 0.0001$; *NS*, not significant (one-way ANOVA and Dunnett's post-test for comparing the various treatments with untreated KO; two-tailed unpaired Student's *t* test for comparing WT mice with resolution *versus* WT mice without resolution, as well as KO mice with resolution *versus* KO mice without resolution).

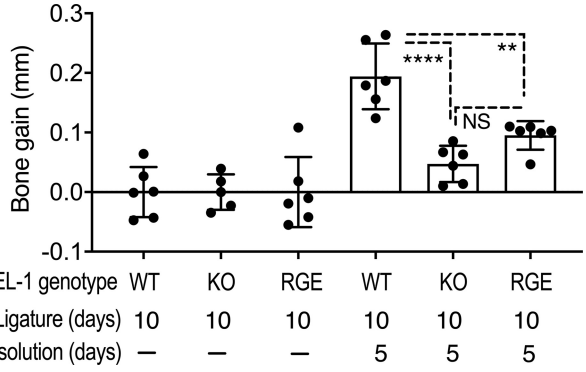


**Figure 4. The ability of DEL-1 to promote bone gain during resolution depends on the RGD motif.** WT, *Del1*$^{KO}$ mice, and *Del1*$^{RGE/RGE}$ mice (8–10 weeks old) were subjected to LIP for 10 days, followed (or not) by 5 days of resolution. Bone regeneration on day 15 was calculated relative to the bone height at day 10, which was taken as the baseline (CEJ–ABC data were transformed to indicate bone gain as outlined in Fig. 1). Data are means ± S.D. (*error bars*) ($n$ = 6 mice/group). **, $p < 0.01$; ****, $p < 0.0001$; *NS*, not significant (one-way ANOVA and Tukey's post-test).

### *DEL-1 promotes Runx2 expression and osteogenic differentiation of MC3T3-E1 cells in a manner dependent on β3 integrin, FAK, and ERK1/2*

We next examined whether the capacity of DEL-1 to promote *in vivo* bone regeneration involves a direct $\beta 3$ integrin–dependent effect on osteoegenesis. To investigate this possibility, we used the clonal osteoprogenitor murine cell line MC3T3-E1. MC3T3-E1 cells display similar regulation of gene expression as human osteoblast progenitors and are widely used as a model to study osteoblast differentiation in a process that displays characteristics analogous to *in vivo* bone formation (36–42). As DEL-1 was earlier shown to interact with the RGD-binding $\beta 3$ integrin (1, 4, 5) and the RGD motif of DEL-1

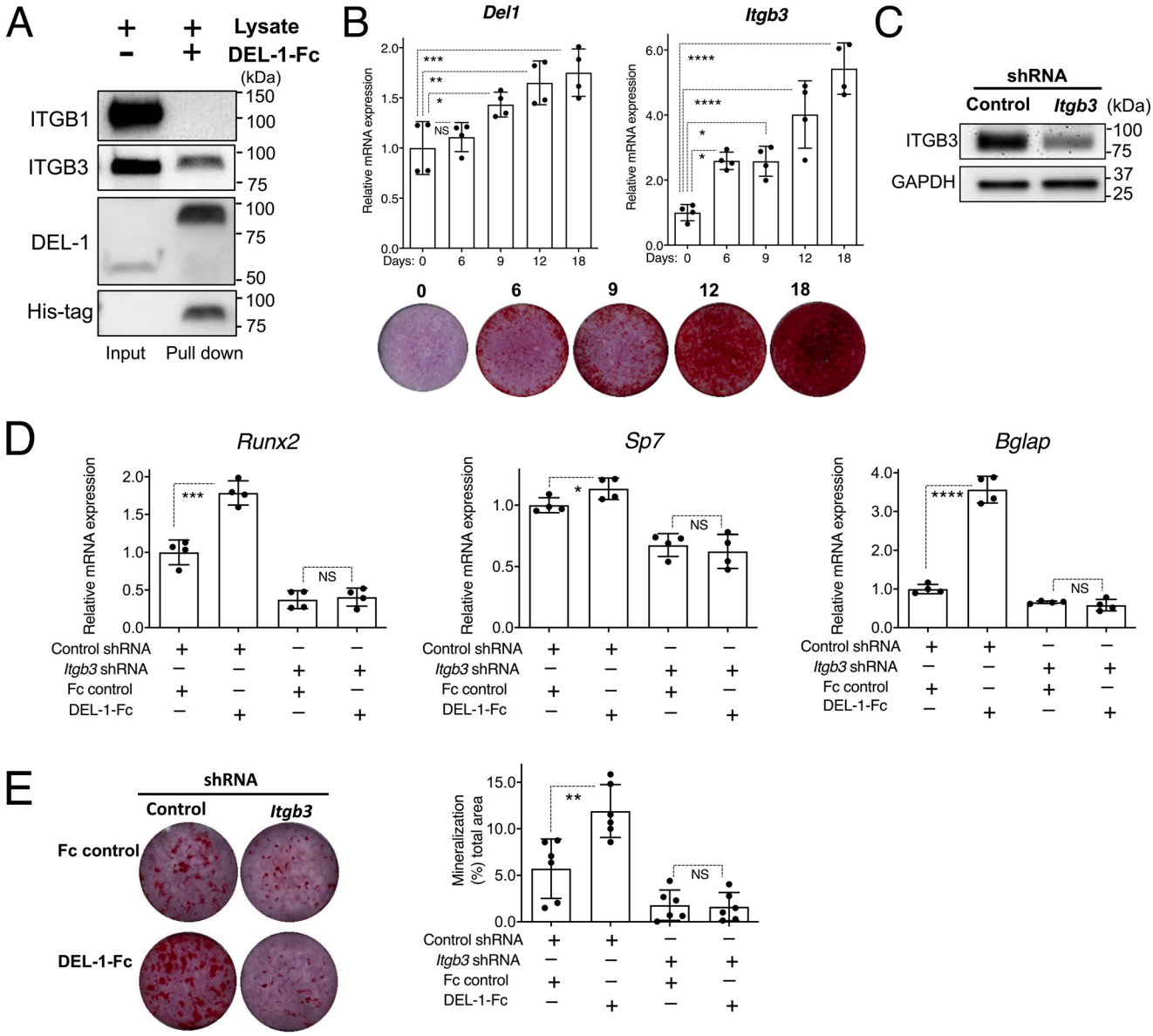


**Figure 5. DEL-1 promotes osteogenic differentiation and mineralization in a β3 integrin–dependent manner.** *A*, His-tagged DEL-1-Fc bound to cobalt-agarose beads was incubated with cell membrane protein lysates from MC3T3-E1 cells, and pulled-down proteins were analyzed by immunoblotting using antibodies to β1 and β3 integrins. Input (10%) represents lysates directly subjected to immunoblotting. DEL-1-Fc was 82 kDa, and endogenous DEL-1 was 52 kDa. *B*, expression of *Del1* and β3 integrin (*Itgb3*) in MC3T3-E1 cells cultured in osteogenic medium at the indicated time points determined by qPCR. Shown in the *bottom panel* is mineralization nodule formation in MC3T3-E1 cultures in osteogenic medium at the same time points. *C–E*, control or β3 integrin shRNA-transfected MC3T3-E1 cells were cultured in osteogenic medium with DEL-1-Fc (2 μg/ml) or an equal molar concentration of Fc control. *C*, knockdown of β3 integrin (ITGB3) confirmed by immunoblotting. *D*, analysis of expression of *Runx2* (day 6), *Sp7* (day 9), *Bglap* (day 12), typical early, middle, and late osteogenic markers, respectively, using qPCR. Data were normalized to *Gapdh* mRNA and expressed relative to Fc-treated and control shRNA-transfected cells, set as 1. *E*, representative images of mineralized nodule formation, detected by Alizarin Red S staining, after 12 days; the *right side* shows quantified results. Data are means ± S.D. (*error bars*) ($n = 4$ (B and D) or $n = 6$ (*E*) cell cultures/group). *, $p < 0.05$; **, $p < 0.01$; ***, $p < 0.001$; ****, $p < 0.0001$; *NS*, not significant (*B*, one-way ANOVA and Dunnett's post-test; *D* and *E*, two-tailed unpaired Student's *t* test).

is essential for its *in vivo* bone regeneration effect (Figs. 3 and 4), we first examined whether DEL-1 can bind β3 integrin from MC3T3-E1 cells. Using a pulldown assay, we showed that DEL-1 can indeed bind β3 integrin, although it failed to bind β1 integrin in the MC3T3-E1 cell lysates (Fig. 5*A*). The expression of β3 integrin increases during osteoblastic differentiation (43). We confirmed this finding using MC3T3-E1 cells cultured in osteogenic medium and, moreover, showed that DEL-1 expression is progressively increased in this system in parallel with increased matrix mineralization (Fig. 5*B*). In MC3T3-E1 cells, DEL-1-Fc induced the expression of the master osteogenic transcription factor *Runx2*, *Sp7* (osterix), and *Bglap* (bone γ-carboxyglutamic acid–containing protein; osteocalcin), typical early, middle, and late osteogenic markers, respectively, as compared with Fc control; however, these up-regulatory effects of DEL-1-Fc were abrogated upon shRNA-mediated β3 integrin knockdown (Fig. 5, *C* and *D*). Moreover, MC3T3-E1 cells cultured in osteogenic medium exhibited increased mineralized nodule formation in the presence of DEL-1-Fc as compared with Fc control, whereas the DEL-1-Fc–induced mineralization activity was blocked in β3 integrin shRNA-transfected cells (Fig. 5*E*). These findings suggest that DEL-1 interacts with

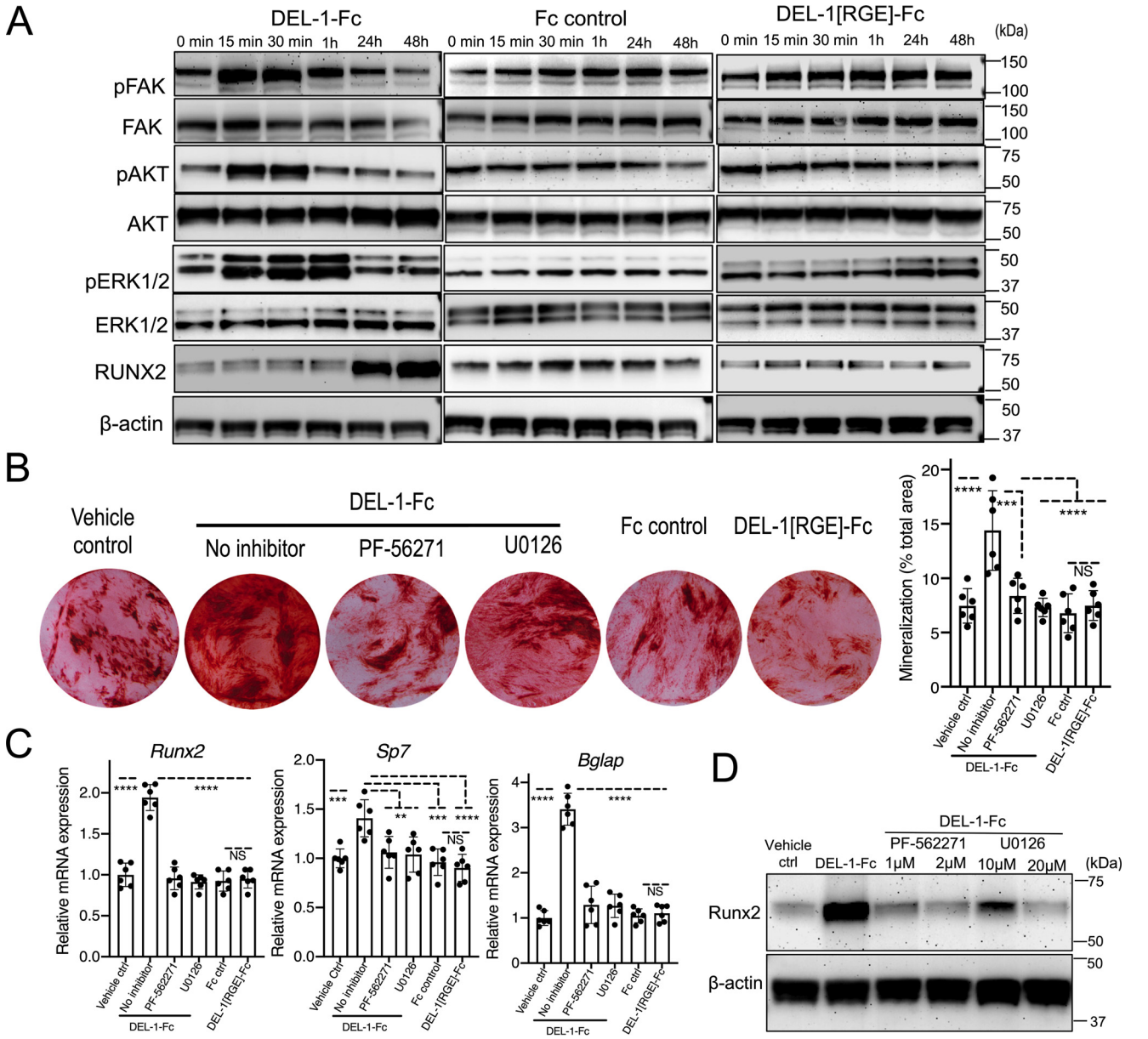


**Figure 6. DEL-1 promotes osteogenic differentiation and mineralization in a manner dependent on FAK and ERK1/2.** *A*, MC3T3-E1 osteoblastic progenitor cells were incubated in growth medium with 1 $\mu$g/ml DEL-1-Fc or DEL-1[RGE]-Fc or equal molar concentration of Fc control for the indicated times. Immunoblot analysis was performed with specific antibodies against phosphorylated and total FAK, AKT, and ERK1/2 as well as against *Runx2* and $\beta$-actin (loading control). *B* and *C*, MC3T3-E1 cells were cultured in osteogenic medium in the presence or DEL-1-Fc (1 $\mu$g/ml) or equal molar amounts of Fc control, DEL-1[RGE]-Fc, or DEL-1[E1–3]-Fc. In some DEL-1-Fc–treated groups, the cells were pretreated with PF-562271 (1 $\mu$M) or U0126 (10 $\mu$M); these inhibitors were added 1 h prior to DEL-1-Fc. Medium was changed every 3 days and was supplemented, as appropriate, with fresh DEL-1-Fc (or mutants/controls thereof) in the presence or absence of fresh signaling inhibitors. Shown are representative images of mineralized nodule formation, detected by Alizarin Red S staining, at day 15 of differentiation (*B*, left) and the mineralization area in each culture quantified and expressed as a percentage of the total area (*B*, *right*). *C*, analysis of MC3T3-E1 cells (treated as in *B*) for the expression of *Runx2* (at day 6), *Sp7* (at day 9), and *Bglap* (at day 12), typical early, middle, and late osteogenic markers, respectively, using qPCR. Data were normalized to *Gapdh* mRNA and expressed relative to medium-only–treated control, set as 1. *D*, Western blot analysis of *Runx2* protein expression at 48 h in MC3T3-E1 cells, incubated in growth medium treated with DEL-1-Fc, in the presence or absence of the indicated concentrations of U0126 or PF-562271, which were added 1 h earlier than DEL-1-Fc. Numerical data are means ± S.D. (*error bars*) ($n = 6$ cultures/group). **, $p < 0.01$; ***, $p < 0.001$; ****, $p < 0.0001$; *NS*, nonsignificant (one-way ANOVA and Tuckey's post-test).

$\beta$3 integrin on MC3T3-E1 osteoblast progenitors and enhances their differentiation to bone-forming cells.

The extracellular matrix plays a major role in the osteogenic differentiation of progenitor cells (21, 22, 44). In human and mouse osteoprogenitors (including MC3T3-E1 cells), extracellular matrix–integrin interactions stimulate recruitment and phosphorylation of FAK followed by activation (phosphorylation) of the key signaling protein ERK1/2, which mediates osteogenic differentiation by enhancing the expression of *Runx2* (25, 26, 45–47). Moreover, FAK activation induces phosphorylation and activation of AKT, which promotes cell survival (46, 48). Using MC3T3-E1 cells, we demonstrated that DEL-1-Fc (but not Fc control) induced phosphorylation of FAK, AKT, and ERK1/2 (within 15 min) and, moreover, induced the expression of *Runx2* protein after 24 h (Fig. 6*A*, *left* and *middle*). Consistent with our earlier data implicating the $\beta$3

integrin in the osteogenic activity of DEL-1 (Fig. 5, *D* and *E*), the point mutant DEL-1[RGE]-Fc (5, 14) that cannot bind β3 integrin failed to induce the phosphorylation of the aforementioned signaling molecules or the expression of *Runx2* (Fig. 6*A*, *right*). Thus, as a secreted protein that associates with the extracellular matrix, DEL-1 can induce signaling consistent with osteogenic differentiation.

Additional evidence implicating the β3 integrin–induced FAK-ERK1/2 signaling pathway in the osteogenic activity of DEL-1 was obtained by showing that the ability of DEL-1-Fc to promote mineralized nodule formation in the MC3T3-E1 system was blocked by inhibitors of FAK (PF-562271) or ERK1/2 (U0126) or when DEL-1[RGE]-Fc was used in lieu of the WT molecule (Fig. 6*B*). Mineralized nodule formation in the presence of DEL-1[RGE]-Fc was similar to Fc control (Fig. 6*B*), suggesting that the integrin-binding RGD motif of DEL-1 is required for its osteogenic activity, as earlier seen *in vivo* (bone regeneration experiments; Figs. 3 and 4). Consistently, the aforementioned signaling inhibitors (PF-562271 and U0126) blocked the ability of DEL-1-Fc to up-regulate the mRNA expression of *Runx2*, *Sp7* (osterix), and *Bglap* (osteocalcin) in MC3T3-E1 osteoblast progenitors. In the presence of PF-562271 or U0126, the expression of the aforementioned osteogenic markers in DEL-1-Fc–treated cells was indistinguishable from that seen in Fc control– or DEL-1[RGE]-Fc–treated cells (Fig. 6*C*). In line with the mRNA data for the master osteogenic transcription factor *Runx2* (Fig. 6*C*, *left*), the capacity of DEL-1 to induce the expression of *Runx2* protein in MC3T3-E1 cells at the 48-h time point was blocked by inhibitors of FAK (PF-562271) or ERK1/2 (U0126) (Fig. 6*D*). Therefore, FAK and ERK1/2 mediate the effect of DEL-1 to enhance the expression of *Runx2* and promote the osteogenic differentiation of MC3T3-E1 osteoblast progenitors.

### *Endogenous DEL-1 promotes osteogenic differentiation of primary calvarial osteoblastic cells through its RGD motif*

To confirm and expand on the data with the MC3T3-E1 cell line treated with exogenous DEL-1 (Figs. 5 and 6), we examined the role of endogenous DEL-1 in primary calvarial osteoblast differentiation by isolating cells from the calvariae of 3-day-old WT, *Del1*$^{KO}$, and *Del1*$^{RGE/RGE}$ mice. When cultured in osteogenic medium, primary calvarial osteoblastic cells lacking DEL-1 expression, or expressing the RGE point mutant, were relatively defective in mineralized nodule formation as compared with WT cells (Fig. 7*A*, *medium-only column*). Indeed, the WT group displayed an almost 3-fold higher mineralization capacity than the *Del1*$^{KO}$ and *Del1*$^{RGE/RGE}$ groups (Fig. 7*B*, *left panel*), suggesting the importance of endogenous intact DEL-1 in optimal osteogenic differentiation. Consistently, exogenously added DEL-1-Fc (but not Fc control) rescued the impaired mineralization capacity of *Del1*$^{KO}$ or *Del1*$^{RGE/RGE}$ calvarial cells, which became comparable with that of WT calvarial cells (Fig. 7, *A* and *B*). Importantly, DEL-1[E1–3]-Fc, but not DEL-1[RGE]-Fc, reproduced the effect of DEL-1-Fc in restoring the mineralization capacity of the *Del1*$^{KO}$ and *Del1*$^{RGE/RGE}$ groups to levels comparable with that of the WT group (Fig. 7, *A* and *B*). In line with the mineralized nodule formation findings, calvarial cells lacking endogenous DEL-1 or expressing the RGE mutant exhibited reduced constitutive expression of *Runx2*, *Sp7*, and *Bglap* mRNA, as compared with WT cells (Fig. 7*C*, medium-only groups; note that, for each gene, all data were normalized to medium-only–treated WT control set as 1). However, the expression of these osteogenic markers was up-regulated by the addition of exogenous DEL-1-Fc or DEL-1[E1–3]-Fc, but not of DEL-1[RGE]-Fc or Fc control (Fig. 7*C*). To further confirm the involvement of β3 integrin in the osteogenic effects of DEL-1, as suggested by the β3 integrin knockdown approach in M3CT3-E1 cells (Fig. 5, *D* and *E*), we used cilengitide, a cyclic RGD peptide that antagonizes αvβ3 integrin (5, 49, 50). Cilengitide inhibited, in a dose-dependent manner, DEL-1–induced mineralized nodule formation (Fig. 7, *D* and *E*) and induction of mRNA expression of osteogenic genes (*Runx2*, *Sp7*, and *Bglap*) (Fig. 7*F*) in primary calvarial osteoblast progenitors. A control peptide had no effect in the same assays (Fig. 7, *D–F*). In line with these findings, the ability of DEL-1 to induce the expression of *Runx2* protein in primary calvarial osteoblast progenitors was blocked dose-dependently by cilengitide (but not by control peptide) (Fig. 7*G*). Taken together, these data show that DEL-1 promotes *Runx2* expression and osteogenic differentiation of primary calvarial osteoblastic cells via a β3 integrin– dependent mechanism that requires its RGD motif but not its C-terminal discoidin-like domains, consistent with the ability of DEL-1[E1–3]-Fc, but not of DEL-1[RGE]-Fc, to promote *in vivo* bone regeneration (Fig. 3).

## Discussion

In this paper, we have shown that endogenous DEL-1 is required for effective bone regeneration during the resolution of experimental periodontitis. Moreover, exogenous DEL-1 could rescue the impaired bone regeneration capacity of DEL-1– deficient mice, suggesting novel therapeutic applications for DEL-1. The present study is, to the best of our knowledge, the first to show that DEL-1 induces new bone formation *in vivo*, consistent with earlier *in vitro* observations linking DEL-1 to osteoblast biology (5, 6). In this regard, we previously showed that DEL-1 mRNA is expressed by cells of the osteoblastic lineage in the mouse bone marrow as well as by primary human osteoblasts (5). Moreover, an independent study, by Oh *et al.* (6), demonstrated DEL-1 mRNA expression in calvaria and tibia/femur bones as well as in MC3T3-E1 osteoprogenitor cells.

The study by Oh *et al.* (6) further reported that the α5β1 integrin mediates DEL-1–induced osteogenic differentiation of MC3T3-E1 osteoprogenitor cells. Although this finding appears to contradict our results showing a strict requirement for β3 integrin in the osteogenic differentiation of MC3T3-E1 cells, it should be noted that Oh *et al.* (6) found that DEL-1–induced matrix mineralization was inhibited equally well by antibodies to either α5β1 or αvβ3 integrin. Knockdown of β3 integrin (which may be a more direct approach to test integrin function than antibody blockade) prevented the ability of DEL-1 to induce expression of osteogenic markers (including the master transcription factor *Runx2*) and to promote matrix mineralization. In line with this, cilengitide, a cyclized RGD-containing peptide that antagonizes αvβ3 integrin (49, 50), blocked *Runx2* mRNA and protein expression. Moreover, we demonstrated direct binding of DEL-1 to β3 integrin, whereas

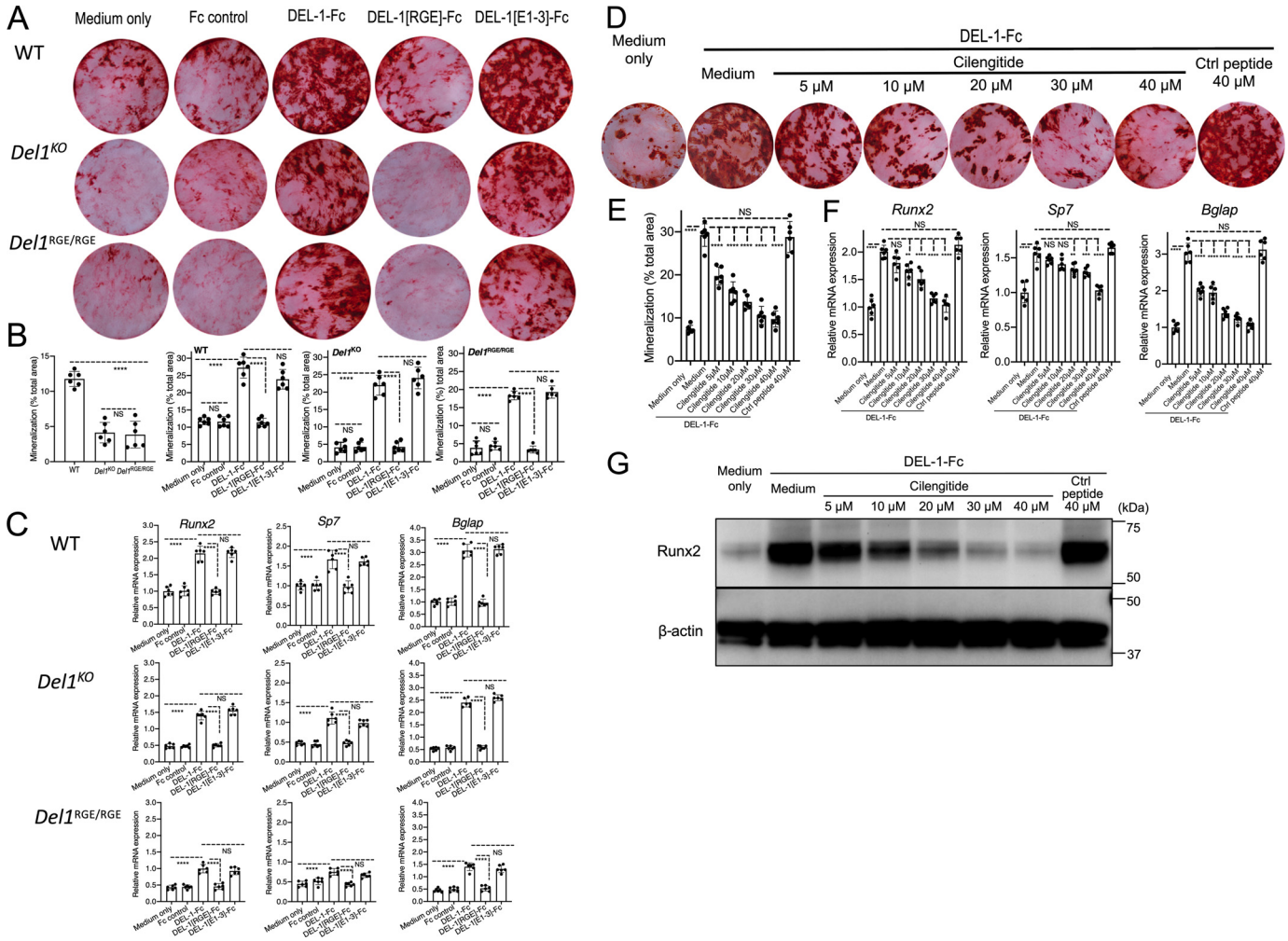


**Figure 7. Endogenous DEL-1 induces osteogenic differentiation in primary calvarial osteoblast progenitors through its RGD motif.** Primary osteoblastic progenitor cells were isolated from the calvariae of 3-day-old WT, *Del1*$^{KO}$, or *Del1*$^{RGE/RGE}$ mice. The cells were cultured in osteogenic medium in the presence (or not) of DEL-1-Fc (1 $\mu$g/ml) or equal molar amounts of Fc control, DEL-1[RGE]-Fc, or DEL-1[E1–3]-Fc and were compared for mineralized nodule formation (*A* and *B*) and osteogenic gene expression (*C*). Shown are representative images of mineralized nodule formation, detected by Alizarin Red S staining, on day 15 of differentiation (*A*) and mineralization area in each culture quantified and expressed as a percentage of the total area (*B*). *C*, primary calvarial osteoblast progenitors from the same strains of mice, treated similarly as above, were assayed by qPCR for expression of *Runx2* (at day 6), *Sp7* (at day 9), and *Bglap* (at day 12), typical early, middle, and late osteogenic markers, respectively. Data were normalized to *Gapdh* mRNA and expressed relative to the medium-only–treated groups of the WT cells, set as 1. *D–G*, primary osteoblastic progenitor cells, isolated from the calvariae of 3-day-old WT mice, were cultured in osteogenic medium in the presence (or not) of DEL-1-Fc (1 $\mu$g/ml) with or without cilengitide (5, 10, 20, 30, or 40 $\mu$M) or 40 $\mu$M RGD control peptide and assayed for mineralization nodule formation (*D* and *E*) and osteogenic gene expression (*F*). Shown are representative images of mineralized nodule formation, detected by Alizarin Red S staining, on day 15 of differentiation (*D*), and the mineralization area in each culture was quantified and expressed as a percentage of the total area (*E*). *F*, primary calvarial osteoblast progenitors from WT mice were treated as above and assayed by qPCR for expression of *Runx2* (at day 6), *Sp7* (at day 9), and *Bglap* (at day 12), respectively. Data were normalized to *Gapdh* mRNA and expressed relative to the control peptide-only–treated group, set as 1. *G*, Western blot analysis of *Runx2* protein expression at 48 h in WT primary osteoblastic progenitor cells incubated in growth medium in the presence (or not) of DEL-1-Fc (1 $\mu$g/ml) with cilengitide (5, 10, 20, 30, and 40 $\mu$M) or control peptide (40 $\mu$M), which were added 1 h earlier than DEL-1-Fc. $\beta$-Actin served as loading control. Data are means ± S.D. (*error bars*) ($n = 6$ cultures/group). **, $p < 0.01$; ***, $p < 0.001$; ****, $p < 0.0001$; *NS*, nonsignificant (one-way ANOVA and Tukey's post-test).

$\beta$1 integrin failed to interact with DEL-1. Thus, in our hands, DEL-1 interacts with $\beta$3 integrin on MC3T3-E1 osteoprogenitor cells and promotes their osteogenic differentiation. In agreement with Oh *et al.* (6), we showed that DEL-1 induces phosphorylation of ERK1/2 followed by increased expression of *Runx2* and, additionally, showed that DEL-1 induces phosphorylation of FAK, a key upstream component of integrin-triggered signal transduction (51). As FAK-mediated AKT activation suppresses apoptosis (46, 48, 52), DEL-1–mediated AKT activation may contribute to enhanced bone formation through increased survival of mature osteoblasts. Moreover, AKT signaling increases the DNA-binding capacity of *Runx2* and *Runx2*-dependent transcription (53). Importantly, upon pharmacologic blockade of FAK and ERK1/2, DEL-1 lost the ability to induce *Runx2* expression and mineralized nodule formation. Overall, our findings suggest that the *in vitro* osteogenic activity of DEL-1 involves a $\beta$3 integrin–FAK–ERK1/2–*Runx2* axis.

To rigorously test the biological relevance of the observations in the MC3T3-E1 cell line system, we used primary calvarial cells from 3-day-old WT, *Del1*$^{KO}$, and *Del1*$^{RGE/RGE}$ mice in similar assays. These experiments not only demonstrated the importance of endogenously produced DEL-1 for optimal osteogenic differentiation of the calvarial cells but unequivocally showed that the integrin-binding RGD motif of endoge-

nous DEL-1 is absolutely required for its osteogenic activity. The osteogenic differentiation of calvarial cells lacking endogenous DEL-1 or expressing an RGE point mutant of DEL-1 was restored upon supplementation with DEL-1-Fc or with DEL-1[E1-E3]-Fc, indicating that the N-terminal segment of DEL-1 that contains the RGD motif (present in the E2 repeat), but lacks the discoidin-like domains, is sufficient to stimulate osteogenic differentiation. These data consistently reflect our *in vivo* findings that DEL-1 promotes bone regeneration during periodontitis resolution via a mechanism that requires its RGD motif but not its C-terminal discoidin-like domains. The requirement for intact RGD motif was established not only by restoring bone regeneration in *Del1*$^{KO}$ mice when given DEL-1-Fc albeit not DEL-1[RGE]-Fc, but also by demonstrating that *Del1*$^{RGE/RGE}$ mice exhibited a similar phenotype (defective bone regeneration) with *Del1*$^{KO}$ mice.

The ability of DEL-1 to promote inflammation resolution through $\beta$3 integrin–mediated apoptotic cell efferocytosis, as we showed recently (4), may secondarily enhance osteoblast function and bone formation (54). However, the efferocytosis mechanism cannot adequately explain the *in vivo* capacity of DEL-1 to promote bone gain during resolution, because efferocytosis also requires the participation of the C-terminal discoidin-like domains of DEL-1, which bind with high-affinity phosphatidylserine, a major "eat-me" signal on the apoptotic cell surface (4, 7). On the other hand, the N-terminal segment of DEL-1 containing the EGF-like repeats and the RGD motif is sufficient to promote bone regeneration *in vivo* and to induce osteoblastic differentiation of progenitor cells *in vitro*; these findings therefore indicate that the novel function of DEL-1 to promote *in vivo* bone regeneration may, at least in part, involve a direct effect on osteogenesis.

Intriguingly, DEL-1 (also known as EDIL3, for epidermal growth factor-like repeats and discoidin I-like domain-3) is among the top six genes most down-regulated by knockdown of *Runx2* in MC3T3-E1 cells undergoing osteoblastic differentiation (55). Because, moreover, DEL-1 up-regulates *Runx2*, it is possible that DEL-1 and *Runx2* might engage in a regulatory loop in which their expression is reciprocally reinforced, thereby promoting osteoblastic differentiation. A proteomic study identified DEL-1 (EDIL3) as a candidate extracellular matrix protein for the regulation of initiation of eggshell calcification (56). In this regard, the fact that the EGF-like repeats of DEL-1 are calcium ion–binding domains strongly suggests that DEL-1, and particularly its N-terminal segment, might play a significant role in calcification. Thus, the N-terminal segment of DEL-1 not only contains an RGD motif that promotes osteoblastic differentiation but contains calcium ion-binding domains that might participate in the mineralization process during bone regeneration.

Periodontitis, an oral inflammatory disease characterized by loss of bone support of the dentition, remains a serious public health and economic burden (15, 57, 58). We have previously shown that endogenous DEL-1 inhibits alveolar bone loss caused by the periodontal microbiota; however, it does not appear to regulate skeletal bone homeostasis at steady state, as *Del1*$^{KO}$ mice develop alveolar bone loss without becoming overtly osteopenic with regard to the long bones or spine (13). Thus, DEL-1 seems to regulate bone levels in sites under stressful stimuli (*e.g.* microbial challenge, which is normally absent in the long bones and vertebrae). Consistent with this notion, locally administered DEL-1-Fc inhibits osteoclastogenesis and alveolar bone loss during the inductive phase of experimental periodontitis in nonhuman primates (14). In the present study, we showed that DEL-1 can also regulate bone levels during the resolution phase of periodontitis, presumably by acting on osteoblastic cells. In this regard, progress has been achieved in terms of approaches to restore bone loss (*e.g.* through the use of scaffolds, stem cells, and soluble molecules, such as bone morphogenetic proteins, fibroblast growth factors, and other growth factors); however, regeneration of bone lost due to periodontitis is of limited success and not predictable (59–61). One of the issues associated with current approaches is that they might not sufficiently control inflammation, which can compromise the regeneration process. By possessing both anti-inflammatory/pro-resolving, and osteogenic properties (4, 6, 8, 13) (and the current paper), DEL-1 could be a novel therapeutic agent capable of contributing to bone regeneration in periodontitis and perhaps other inflammation-driven osteolytic disorders.

DEL-1 was shown to protect against inflammatory pathologies, including bone loss, in mice and nonhuman primates, and the results from these models are consistent with human clinical observations; this is not surprising, given that human DEL-1 has ≥96% amino acid sequence identity with its mouse and nonhuman primate counterparts (4, 8, 11, 13, 14, 62, 63). Moreover, DEL-1 expression is regulated similarly in humans and mice (11), and DEL-1 is highly expressed by both human and mouse osteoblastic cells (5, 6) (and the present study). Therefore, our finding that DEL-1 promotes bone regeneration during resolution of mouse periodontitis is likely to be relevant for the treatment of human periodontitis. To date, most therapeutic strategies targeting integrin function involve inhibitors that block ligand binding or downstream signaling, whereas molecules that induce beneficial responses by binding integrins (*e.g.* DEL-1 binding to $\beta$3 integrin to promote bone regeneration) have yet to be developed for clinical use (64).

## Experimental procedures

### *Mice*

The generation of C57BL/6 *Edil3*$^{-/-}$ (*Del1*$^{KO}$) mice was described previously (8). The generation of *Del1*$^{RGE/RGE}$ mice (which express a point mutant of DEL-1 incapable of interacting with the $\alpha v\beta 3$ integrin) is described in detail below. *Del1*$^{KO}$ and *Del1*$^{RGE/RGE}$ mice were crossed with WT C57BL/6 mice to generate experimental mice and WT littermate controls. In experiments where only WT C57BL/6 mice were used, these were purchased from the Jackson Laboratory (Bar Harbor, ME) (catalog no. 000664). Sex- and age-matched mice (8–10 weeks old) were used in *in vivo* experiments; as there were no significant differences in the data obtained using male or female mice, the results were pooled per treatment group. Mice were maintained in individually ventilated cages under specific pathogen-free conditions on a standard 12-h light/dark cycle. Food and water were provided *ad libitum*. All animal experiments were

reviewed and approved by the Institutional Animal Care and Use Committee of the University of Pennsylvania and were performed in compliance with institutional, state, and federal policies.

### Generation of *Del1*$^{RGE/RGE}$ mice

*Del1*$^{RGE/RGE}$ mice that express the RGE point mutant of DEL-1 (DEL-1$^{RGD98E}$) were generated using one-step CRISPR/Cas-mediated genome editing (65, 66). Briefly, zygotes from C57BL/6 mice were co-injected with Cas9 mRNA (65) and the designed sgRNA (UAUCGAGGAGACACAUUCAUGUUUUAGAGCUAGAAAUAGCAAGUUAAAAUAAGGCUAGUCCGUUAUCAACUUGAAAAAGUGGCACCGAGUCGGUGCUUUUUU) in combination with donor ssDNA oligonucleotides (t*t*t*cagGTCCCTGCATCCCTAACCCATGCCATAACGGAGGAACCTGTGAGATAAGCGAAGCCTATCGAGGAGAGACGTTTATAGGCTATGTTTGTAAATGTCCTCGGGGATTTAATGGGATTCACTGTCAGCACAgtaagtta*t*t*t) (67). The sgRNA was designed and prepared using the rules outlined previously (67, 68). RGD motif-coding sequences in the DEL-1–encoding *EDIL3* gene, CGAGGAGAC, contain a proto-spacer adjacent motif sequence, AGG. Therefore, 20 nucleotide bases preceding the sequence AGG, TATCGAGGAGACACATTCA, were selected as the target of CRISPR RNAs (crRNAs). crRNA sequences were then fused to the trans-activating crRNA (69) that binds and stabilizes the Cas9 nuclease to get sgRNA. In zygotes, Cas9 protein generated double-strand break within the target DNA directed by sgRNA. The host DNA repair machinery performed the homology-directed repair using the ssDNA oligonucleotide (with short homology (70 nucleotides) flanking the double-strand break from each direction) as a template to induce a point mutation into the *EDIL3* gene. Blastocysts were then implanted into foster mothers to obtain pups with mutations. The RGE point mutation was confirmed by Sanger sequencing and by a specific set of primers that capture the targeted mutation. The sequences of primers were as follows: P1, forward primer 1 for WT-RGD (P1-WT-RGD-F, 5′-AGCCTATCGAGGAGACACATTC-3′); P2, forward primer 2 for RGE (P2- RGE-F, 5′-AGCCTATCGAGGAGAGACGTTT-3′); and P3, common reverse primer (P3-R, 5′-CCAAAATGCCTAGACTCGGTGCC-3′). DNA was denatured at 95 °C for 4 min and then amplified by 30 cycles at 95 °C for 1 min, 62 °C for 1 min, and 72 °C for 1 min. Homozygote mice with RGE mutation were backcrossed to WT C57BL/6 mice to generate heterozygotes to minimize unwanted gene modifications, which were bred to generate a homozygote colony. The colony is viable and breeds normally.

### DEL-1 and mutants thereof and other reagents

Full-length human DEL-1 as a fusion protein with the human IgG1-Fc fragment (DEL-1-Fc), DEL-1 lacking the discoidin I-like domains (DEL-1[E1-E3]-Fc), and a point mutant of DEL-1 in which Asp was replaced by Glu in the RGD motif of the second EGF repeat (DEL-1[RGE]-Fc) were generated and purified as described previously (14). Fc protein control was purchased from R&D Systems (Minneapolis, MN) (catalog no. 110-HG-100). As human and mouse DEL-1 share 96% amino acid sequence and the two proteins have similar functions (4, 8, 13, 14), human DEL-1 was used in mouse experimental systems in the current study, as in previous publications (4, 5, 14). Cilengitide, a cyclic RGD peptide that inhibits $\alpha v\beta 3$ integrin (5, 49, 50) was purchased from Selleck Chemicals (Houston, TX) (catalog no. S7077) and RGD control peptide (GRADSP) from Enzo Life Sciences (Farmingdale, NY) (catalog no. BML-P701-0005). The FAK inhibitor PF-562271 (70) was obtained from Selleck Chemicals (catalog no. S2890), and the selective MEK/ERK inhibitor U0126 (71) was from Invivogen (San Diego, CA) (catalog no. tlrl-u0126).

### Resolution of ligature-induced periodontitis and intervention experiments

Groups of 8-week-old mice were subjected to experimental periodontitis by tying a 5-0 silk ligature around the maxillary left second molar for 10 days. The contralateral tooth was kept unligated as a baseline control. To enable periodontitis resolution, the ligatures were removed at day 10, and the mice were sacrificed 5 days later (at day 15). Periodontal bone loss was assessed morphometrically in defleshed maxillae using a dissecting microscope (×40) equipped with a video image measurement system (Nikon Instruments, Melville, NY). Specifically, the distance from the cement-enamel junction (CEJ) to the alveolar bone crest (ABC) was measured on six predetermined points on the ligated second molar and the affected adjacent regions (17). Bone loss was calculated by subtracting the six-site total CEJ–ABC distance of the ligated side of each mouse from the six-site total CEJ–ABC distance on the contralateral unligated side. The data were further transformed to indicate bone gain (or loss; negative value) relative to the bone levels of mice that were sacrificed at day 10 (see Fig. 1*D*). To study the role of DEL-1 in bone regeneration during the resolution phase, mice were daily microinjected (at days 10–14) with Fc control (0.33 $\mu$g; 12.3 pmol) and various versions of DEL-1 at molar equivalents: intact DEL-1-Fc (1 $\mu$g), DEL-1[RGE]-Fc (1 $\mu$g), and DEL-1[E1–3]-Fc (0.54 $\mu$g). Microinjections were performed into the palatal gingiva between first and second maxillary molars using a 33-gauge stainless steel needle attached to a Hamilton microsyringe (Fisher, catalog no. 7633-01).

### Histology

Coronal sections of the ligated molars were prepared and stained with modified Masson's trichrome staining kit (Abcam (Cambridge, MA), catalog no. ab150686), which stains mature (old) bone and connective tissue in blue, whereas it stains immature new bone (osteoid) and collagen in red (72).

### Osteoblastic progenitors

The murine osteoblastic progenitor cell line (MC3T3-E1 subclone 4) was purchased from ATCC (Manassas, VA) (catalog no. CRL-2593). Primary cultures of osteoblastic progenitor cells were derived from 3-day-old WT, *Del1*$^{KO}$, and *Del1*$^{RGE/RGE}$ mice by digesting calvarias in PBS containing 0.1% collagenase Type I (Worthington, catalog no. LS004216) and 0.2% ROCHE Dispase II (MilliporeSigma, catalog no. 50-100-3345) for 20 min at

37 °C. The digestion was sequentially performed three times, and cells isolated from the last two digestions were cultured in α-minimum essential medium (α-MEM; Fisher, catalog no. 32-561-037) supplemented with 10% fetal bovine serum (FBS) as primary osteoblastic progenitors (73, 74). All cells were maintained in α-MEM supplemented with 10% FBS, 50 units/ml penicillin, and 50 μg/ml streptomycin ("growth medium").

### Osteogenic differentiation assay

For osteogenic differentiation, the osteoblastic progenitors were cultured in "osteogenic medium" (50 μg/ml ascorbic acid (catalog no. 1043003, MilliporeSigma) and 10 mM β-glycerophosphate (catalog no. G9422, MilliporeSigma) in α-MEM supplemented with 10% FBS) for up to 15 days (timing specified in the figure legends). The medium, which in some experiments included DEL-1-Fc (or mutants/controls thereof) and inhibitors, was changed every 3 days. Mineralized bone nodules were detected by staining with Alizarin Red S (catalog no. A5533, MilliporeSigma). To this end, the cultures were washed twice with PBS, fixed with 4% paraformaldehyde in PBS for 15 min, and washed again with PBS and sterile water. Staining was performed by covering the cells with 2% Alizarin Red S solution for 45 min followed by extensive rinsing. The plates were scanned, and the calcified nodules were quantified (as percentage of area coverage relative to the total area) using ImageJ software.

### Quantitative real-time PCR (qPCR)

Total RNA was extracted from cultured cells using TRIzol reagent (Life Technologies, Inc., catalog no. 15596018) according to the manufacturer's instructions. 500 ng of total RNA was reverse-transcribed using the High-Capacity RNA-to-cDNA Kit (Thermo Fisher Scientific, catalog no. 4387406), and real-time PCR with cDNA was performed using the Applied Biosystems 7500 Fast Real-Time PCR System according to the manufacturer's protocol. TaqMan probes and gene-specific primers for detection and quantification of murine genes investigated in this study were purchased from Thermo Fisher Scientific. Data were analyzed using the comparative ($\Delta\Delta Ct$) method. The primers used in this study included *Itgb3* (Mm00443980_m1); *Edil3* (Mm01291247_m1); *Runx2* (Mm00501584_m1); *Bglap* (Mm03413826_mH); *Sp7* (Mm00504574_m1); *Gapdh* (Mm99999915_g1).

### Immunoblotting

Following treatment, cell lysates were prepared using the radioimmune precipitation assay buffer (catalog no. sc-24948, Santa Cruz Biotechnology, Dallas, TX) supplemented with Halt protease and phosphatase inhibitor mixture (catalog no. 78440, Thermo Fisher Scientific). Protein content concentrations were determined using the Bradford protein assay (catalog no. 23200, Thermo Fisher Scientific). The samples were then subjected to SDS-PAGE and subsequently transferred onto a polyvinylidene difluoride membrane (Immobilon-P; catalog no. IPVH00010, MilliporeSigma), blocked with Starting Block (TBS) blocking buffer (catalog no. 37542, Thermo Fisher Scientific), probed with primary antibody (4 °C overnight), and then incubated with corresponding secondary antibodies at room temperature for 1 h. After enhanced chemiluminescence using Luminata Forte Western HRP substrate (catalog no. WBKLS0100, MilliporeSigma), the protein bands were imaged using the FluorChem M imaging system (ProteinSimple, San Jose, CA). Rabbit polyclonal antibodies to FAK (catalog no. 3285), phospho-FAK (Tyr-397; catalog no. 3283), and AKT (catalog no. 9272), as well as rabbit mAbs to phospho-AKT (Ser-473; clone D9E; catalog no. 4060), ERK (clone 137F5; catalog no. 4398), phospho-ERK (Thr-202/Tyr-204; clone D13.14.4E; catalog no. 4370), *Runx2* (clone D1L7F; catalog no. 12556), and β-actin (clone 13E5; catalog no. 4970) were purchased from Cell Signaling Technology (Danvers, MA).

### Pulldown assay

Pulldown experiments were performed using the Pulldown polyHis protein:protein interaction kit (catalog no. 21277, Thermo Fisher Scientific) as per the manufacturer's instructions. Briefly, MC3T3-E1 cells were cultured in a T75 flask at 37 °C for 48 h. After reaching confluence, the cells (~$1 \times 10^7$) were released by trypsin digestion, neutralized with medium containing 10% FBS, washed with PBS, and collected by centrifugation (500 × *g*, 5 min). The cells were then lysed, and the cell membrane proteins were isolated using a cell fractionation kit (catalog no. 9038, Cell Signaling Technology). The pulldown washing solution was prepared by mixing a 1:1 solution of TBS/Thermo Fisher Scientific Lysis Buffer and adding imidazole stock solution (4 M) to a final concentration of 10 mM imidazole. Cobalt chelate resin (50 μl) was added to the spin column and equilibrated with washing solution. Subsequently, the resin was incubated with 300 μl of histidine-tagged DEL-1-Fc (100 μg) at 4 °C with gentle rocking. After incubation for 1 h, the DEL-1-Fc– bonded resins were collected in the spin column by centrifugation (1,250 × *g*, 1 min), washed five times, and incubated with the MC3T3-E1 cell membrane lysate for 4 h at 4 °C. After washing an additional five times, the bound proteins in the resin were eluted with elution buffer containing 290 mM imidazole. The eluted sample was resolved using SDS-PAGE, and the captured molecules were identified by immunoblotting with appropriate antibodies: rabbit mAbs to β3 integrin (clone D7X3P; catalog no. 13166, Cell Signaling Technology) and β1 integrin (clone D6S1W; catalog no. 34971, Cell Signaling Technology), as well as rabbit polyclonal antibody to DEL-1 (polyclonal; catalog no. 12580-1-AP, Proteintech (Rosemont, IL)), and HRP-conjugated murine anti-$His_6$ tag antibody (clone 3D5; catalog no. R931-25, Thermo Fisher Scientific).

### Receptor knockdown by specific shRNA

To knock down integrin β3 in MC3T3-E1 cells, the shRNA pLKO.1 construct specific for integrin β3 (catalog no. TRCN0000009620, MilliporeSigma) was used. Empty pLKO.1 vector (catalog no. SHC001, MilliporeSigma) served as control. Knockdown efficiency was confirmed by immunoblotting using rabbit mAb to β3 integrin. Glyceraldehyde-3-phosphate dehydrogenase (GAPDH), detected by rabbit mAb to GAPDH (clone 14C10; catalog no. 2118, Cell Signaling Technology) was used as loading control. For transfection of shRNA, cells were plated in 6-well plates at a density of $1.5 \times 10^5$ cells/well, cultured until 70–80% confluence, and transfected with vectors

using FuGene HD (catalog no. E2311, Promega, Madison, WI) transfection reagent using a ratio of 4:1 (volume of FuGene/$\mu$g of DNA). Cells were maintained in nonselective medium for 48 h post-transfection and then changed to selection medium containing puromycin (2 $\mu$g/ml; catalog no. A1113802, Thermo Fisher Scientific). The use of selection medium was continued for 3 weeks with frequent changes of medium to eliminate dead cells and debris until distinct colonies could be visualized. The adherent cells were further released by trypsin digestion (TrypLE Select Enzyme; catalog no. 12563011, Thermo Fisher Scientific) and plated in T75 flasks for further propagation. The transfected cells were maintained under selection medium (containing 2 $\mu$g/ml puromycin) for the duration of the experiments.

### Statistical analysis

For the comparison of three or more groups, data were evaluated by one-way ANOVA and Dunnett's or Tukey's multiple-comparison test, as appropriate. Regarding comparison of two groups only, a two-tailed Student's $t$ test was performed. $p < 0.05$ was considered to be statistically significant. GraphPad Prism software (version 8.2.1) (GraphPad Software, San Diego, CA) was used for the statistical analysis.

### Data availability

All data are contained within the manuscript.

*Author contributions*—D.-Y. Y., T. M., and X. L. data curation; D.-Y. Y., T. M., and X. L. formal analysis; D.-Y. Y., T. M., and X. L. validation; D.-Y. Y. and T. M. investigation; D.-Y. Y., X. L., and T. K. methodology; D.-Y. Y. and G. H. writing-original draft; T. K. and K. B. resources; T. C. and G. H. conceptualization; T. C. and G. H. writing-review and editing; G. H. supervision; T. C. and G. H. funding acquisition; G. H. project administration.

## References


1. Hidai, C., Zupancic, T., Penta, K., Mikhail, A., Kawana, M., Quertermous, E. E., Aoka, Y., Fukagawa, M., Matsui, Y., Platika, D., Auerbach, R., Hogan, B. L., Snodgrass, R., and Quertermous, T. (1998) Cloning and characterization of developmental endothelial locus-1: an embryonic endothelial cell protein that binds the $\alpha v\beta 3$ integrin receptor. *Genes Dev.* **12,** 21–33 CrossRef Medline
2. Hidai, C., Kawana, M., Kitano, H., and Kokubun, S. (2007) Discoidin domain of Del1 protein contributes to its deposition in the extracellular matrix. *Cell Tissue Res.* **330,** 83–95 CrossRef Medline
3. Chavakis, E., Choi, E. Y., and Chavakis, T. (2009) Novel aspects in the regulation of the leukocyte adhesion cascade. *Thromb. Haemost.* **102,** 191–197 CrossRef Medline
4. Kourtzelis, I., Li, X., Mitroulis, I., Grosser, D., Kajikawa, T., Wang, B., Grzybek, M., von Renesse, J., Czogalla, A., Troullinaki, M., Ferreira, A., Doreth, C., Ruppova, K., Chen, L. S., Hosur, K., *et al.* (2019) DEL-1 promotes macrophage efferocytosis and clearance of inflammation. *Nat. Immunol.* **20,** 40–49 CrossRef Medline
5. Mitroulis, I., Chen, L.-S., Singh, R. P., Kourtzelis, I., Economopoulou, M., Kajikawa, T., Troullinaki, M., Ziogas, A., Ruppova, K., Hosur, K., Maekawa, T., Wang, B., Subramanian, P., Tonn, T., Verginis, P., *et al.* (2017) Secreted protein Del-1 regulates myelopoiesis in the hematopoietic stem cell niche. *J. Clin. Invest.* **127,** 3624–3639 CrossRef Medline
6. Oh, S. H., Kim, J. W., Kim, Y., Lee, M. N., Kook, M. S., Choi, E. Y., Im, S. Y., and Koh, J. T. (2017) The extracellular matrix protein Edil3 stimulates osteoblast differentiation through the integrin $\alpha 5\beta 1$/ERK/Runx2 pathway. *PLoS ONE* **12,** e0188749 CrossRef Medline
7. Hanayama, R., Tanaka, M., Miwa, K., and Nagata, S. (2004) Expression of developmental endothelial locus-1 in a subset of macrophages for engulfment of apoptotic cells. *J. Immunol.* **172,** 3876–3882 CrossRef Medline
8. Choi, E. Y., Chavakis, E., Czabanka, M. A., Langer, H. F., Fraemohs, L., Economopoulou, M., Kundu, R. K., Orlandi, A., Zheng, Y. Y., Prieto, D. A., Ballantyne, C. M., Constant, S. L., Aird, W. C., Papayannopoulou, T., Gahmberg, C. G., *et al.* (2008) Del-1, an endogenous leukocyte-endothelial adhesion inhibitor, limits inflammatory cell recruitment. *Science* **322,** 1101–1104 CrossRef Medline
9. Mitroulis, I., Kang, Y. Y., Gahmberg, C. G., Siegert, G., Hajishengallis, G., Chavakis, T., and Choi, E. Y. (2014) Developmental endothelial locus-1 attenuates complement-dependent phagocytosis through inhibition of Mac-1-integrin. *Thromb. Haemost.* **111,** 1004–1006 CrossRef Medline
10. Hajishengallis, G., and Chavakis, T. (2019) DEL-1-regulated immune plasticity and inflammatory disorders. *Trends Mol. Med.* **25,** 444–459 CrossRef Medline
11. Maekawa, T., Hosur, K., Abe, T., Kantarci, A., Ziogas, A., Wang, B., Van Dyke, T. E., Chavakis, T., and Hajishengallis, G. (2015) Antagonistic effects of IL-17 and D-resolvins on endothelial Del-1 expression through a GSK-$3\beta$-C/EBP$\beta$ pathway. *Nat. Commun.* **6,** 8272 CrossRef Medline
12. Hajishengallis, G., and Chavakis, T. (2013) Endogenous modulators of inflammatory cell recruitment. *Trends Immunol.* **34,** 1–6 CrossRef Medline
13. Eskan, M. A., Jotwani, R., Abe, T., Chmelar, J., Lim, J. H., Liang, S., Ciero, P. A., Krauss, J. L., Li, F., Rauner, M., Hofbauer, L. C., Choi, E. Y., Chung, K. J., Hashim, A., Curtis, M. A., *et al.* (2012) The leukocyte integrin antagonist Del-1 inhibits IL-17-mediated inflammatory bone loss. *Nat. Immunol.* **13,** 465–473 CrossRef Medline
14. Shin, J., Maekawa, T., Abe, T., Hajishengallis, E., Hosur, K., Pyaram, K., Mitroulis, I., Chavakis, T., and Hajishengallis, G. (2015) DEL-1 restrains osteoclastogenesis and inhibits inflammatory bone loss in nonhuman primates. *Sci. Transl. Med.* **7,** 307ra155 CrossRef Medline
15. Hajishengallis, G. (2015) Periodontitis: from microbial immune subversion to systemic inflammation. *Nat. Rev. Immunol.* **15,** 30–44 CrossRef Medline
16. Eke, P. I., Dye, B. A., Wei, L., Slade, G. D., Thornton-Evans, G. O., Borgnakke, W. S., Taylor, G. W., Page, R. C., Beck, J. D., and Genco, R. J. (2015) Update on prevalence of periodontitis in adults in the United States: NHANES 2009 to 2012. *J. Periodontol.* **86,** 611–622 CrossRef Medline
17. Abe, T., and Hajishengallis, G. (2013) Optimization of the ligature-induced periodontitis model in mice. *J. Immunol. Methods* **394,** 49–54 CrossRef Medline
18. Dutzan, N., Kajikawa, T., Abusleme, L., Greenwell-Wild, T., Zuazo, C. E., Ikeuchi, T., Brenchley, L., Abe, T., Hurabielle, C., Martin, D., Morell, R. J., Freeman, A. F., Lazarevic, V., Trinchieri, G., Diaz, P. I., *et al.* (2018) A dysbiotic microbiome triggers TH17 cells to mediate oral mucosal immunopathology in mice and humans. *Sci. Transl. Med.* **10,** eaat0797 CrossRef Medline
19. Ortega-Gómez, A., Perretti, M., and Soehnlein, O. (2013) Resolution of inflammation: an integrated view. *EMBO Mol. Med.* **5,** 661–674 CrossRef Medline
20. Van Dyke, T. E., Hasturk, H., Kantarci, A., Freire, M. O., Nguyen, D., Dalli, J., and Serhan, C. N. (2015) Proresolving nanomedicines activate bone regeneration in periodontitis. *J. Dent. Res.* **94,** 148–156 CrossRef Medline
21. Dangaria, S. J., Ito, Y., Walker, C., Druzinsky, R., Luan, X., and Diekwisch, T. G. (2009) Extracellular matrix-mediated differentiation of periodontal progenitor cells. *Differentiation* **78,** 79–90 CrossRef Medline
22. Mathews, S., Bhonde, R., Gupta, P. K., and Totey, S. (2012) Extracellular matrix protein mediated regulation of the osteoblast differentiation of bone marrow derived human mesenchymal stem cells. *Differentiation* **84,** 185–192 CrossRef Medline
23. Globus, R. K., Moursi, A., Zimmerman, D., Lull, J., and Damsky, C. (1995) Integrin-extracellular matrix interactions in connective tissue remodeling and osteoblast differentiation. *ASGSB Bull.* **8,** 19–28 Medline
24. Khatiwala, C. B., Peyton, S. R., Metzke, M., and Putnam, A. J. (2007) The regulation of osteogenesis by ECM rigidity in MC3T3-E1 cells requires MAPK activation. *J. Cell Physiol.* **211,** 661–672 CrossRef Medline

25. Ge, C., Yang, Q., Zhao, G., Yu, H., Kirkwood, K. L., and Franceschi, R. T. (2012) Interactions between extracellular signal-regulated kinase 1/2 and p38 MAP kinase pathways in the control of RUNX2 phosphorylation and transcriptional activity. *J. Bone Miner. Res.* **27,** 538–551 CrossRef Medline
26. Marie, P. J., Haÿ, E., and Saidak, Z. (2014) Integrin and cadherin signaling in bone: role and potential therapeutic targets. *Trends Endocrinol. Metab.* **25,** 567–575 CrossRef Medline
27. Hajishengallis, G., Lamont, R. J., and Graves, D. T. (2015) The enduring importance of animal models in understanding periodontal disease. *Virulence* **6,** 229–235 CrossRef Medline
28. Graves, D. T., Fine, D., Teng, Y. T., Van Dyke, T. E., and Hajishengallis, G. (2008) The use of rodent models to investigate host-bacteria interactions related to periodontal diseases. *J. Clin. Periodontol.* **35,** 89–105 CrossRef Medline
29. Jiao, Y., Darzi, Y., Tawaratsumida, K., Marchesan, J. T., Hasegawa, M., Moon, H., Chen, G. Y., Núñez, G., Giannobile, W. V., Raes, J., and Inohara, N. (2013) Induction of bone loss by pathobiont-mediated nod1 signaling in the oral cavity. *Cell Host Microbe* **13,** 595–601 CrossRef Medline
30. Lee, C.-T., Teles, R., Kantarci, A., Chen, T., McCafferty, J., Starr, J. R., Brito, L. C. N., Paster, B. J., and Van Dyke, T. E. (2016) Resolvin E1 reverses experimental periodontitis and dysbiosis. *J. Immunol.* **197,** 2796–2806 CrossRef Medline
31. Sima, C., Gastfreund, S., Sun, C., and Glogauer, M. (2014) Rac-null leukocytes are associated with increased inflammation-mediated alveolar bone loss. *Am. J. Pathol.* **184,** 472–482 CrossRef Medline
32. Glowacki, A. J., Yoshizawa, S., Jhunjhunwala, S., Vieira, A. E., Garlet, G. P., Sfeir, C., and Little, S. R. (2013) Prevention of inflammation-mediated bone loss in murine and canine periodontal disease via recruitment of regulatory lymphocytes. *Proc. Natl. Acad. Sci. U.S.A.* **110,** 18525–18530 CrossRef Medline
33. Rovin, S., Costich, E. R., and Gordon, H. A. (1966) The influence of bacteria and irritation in the initiation of periodontal disease in germfree and conventional rats. *J. Periodontal. Res.* **1,** 193–204 CrossRef Medline
34. Tsukasaki, M., Komatsu, N., Nagashima, K., Nitta, T., Pluemsakunthai, W., Shukunami, C., Iwakura, Y., Nakashima, T., Okamoto, K., and Takayanagi, H. (2018) Host defense against oral microbiota by bone-damaging T cells. *Nat. Commun.* **9,** 701 CrossRef Medline
35. Pacios, S., Kang, J., Galicia, J., Gluck, K., Patel, H., Ovaydi-Mandel, A., Petrov, S., Alawi, F., and Graves, D. T. (2012) Diabetes aggravates periodontitis by limiting repair through enhanced inflammation. *FASEB J.* **26,** 1423–1430 CrossRef Medline
36. Henriquez, B., Hepp, M., Merino, P., Sepulveda, H., van Wijnen, A. J., Lian, J. B., Stein, G. S., Stein, J. L., and Montecino, M. (2011) C/EBP$\beta$ binds the P1 promoter of the Runx2 gene and up-regulates Runx2 transcription in osteoblastic cells. *J. Cell Physiol.* **226,** 3043–3052 CrossRef Medline
37. Czekanska, E. M., Stoddart, M. J., Richards, R. G., and Hayes, J. S. (2012) In search of an osteoblast cell model for *in vitro* research. *Eur. Cell Mater.* **24,** 1–17 CrossRef Medline
38. Hong, D., Chen, H. X., Yu, H. Q., Liang, Y., Wang, C., Lian, Q. Q., Deng, H. T., and Ge, R. S. (2010) Morphological and proteomic analysis of early stage of osteoblast differentiation in osteoblastic progenitor cells. *Exp. Cell Res.* **316,** 2291–2300 CrossRef Medline
39. Kartsogiannis, V., and Ng, K. W. (2004) Cell lines and primary cell cultures in the study of bone cell biology. *Mol. Cell Endocrinol.* **228,** 79–102 CrossRef Medline
40. Quarles, L. D., Yohay, D. A., Lever, L. W., Caton, R., and Wenstrup, R. J. (1992) Distinct proliferative and differentiated stages of murine MC3T3-E1 cells in culture: an *in vitro* model of osteoblast development. *J. Bone Miner. Res.* **7,** 683–692 CrossRef Medline
41. Addison, W. N., Nelea, V., Chicatun, F., Chien, Y. C., Tran-Khanh, N., Buschmann, M. D., Nazhat, S. N., Kaartinen, M. T., Vali, H., Tecklenburg, M. M., Franceschi, R. T., and McKee, M. D. (2015) Extracellular matrix mineralization in murine MC3T3-E1 osteoblast cultures: an ultrastructural, compositional and comparative analysis with mouse bone. *Bone* **71,** 244–256 CrossRef Medline
42. Chandra, A., Lan, S., Zhu, J., Siclari, V. A., and Qin, L. (2013) Epidermal growth factor receptor (EGFR) signaling promotes proliferation and survival in osteoprogenitors by increasing early growth response 2 (EGR2) expression. *J. Biol. Chem.* **288,** 20488–20498 CrossRef Medline
43. Di Benedetto, A., Brunetti, G., Posa, F., Ballini, A., Grassi, F. R., Colaianni, G., Colucci, S., Rossi, E., Cavalcanti-Adam, E. A., Lo Muzio, L., Grano, M., and Mori, G. (2015) Osteogenic differentiation of mesenchymal stem cells from dental bud: role of integrins and cadherins. *Stem Cell Res.* **15,** 618–628 CrossRef Medline
44. Evans, N. D., Gentleman, E., Chen, X., Roberts, C. J., Polak, J. M., and Stevens, M. M. (2010) Extracellular matrix-mediated osteogenic differentiation of murine embryonic stem cells. *Biomaterials* **31,** 3244–3252 CrossRef Medline
45. Saidak, Z., Le Henaff, C., Azzi, S., Marty, C., Da Nascimento, S., Sonnet, P., and Marie, P. J. (2015) Wnt/$\beta$-catenin signaling mediates osteoblast differentiation triggered by peptide-induced $\alpha5\beta1$ integrin priming in mesenchymal skeletal cells. *J. Biol. Chem.* **290,** 6903–6912 CrossRef Medline
46. Marie, P. J. (2013) Targeting integrins to promote bone formation and repair. *Nat. Rev. Endocrinol.* **9,** 288–295 CrossRef Medline
47. Hamidouche, Z., Fromigué, O., Ringe, J., Häupl, T., Vaudin, P., Pagès, J. C., Srouji, S., Livne, E., and Marie, P. J. (2009) Priming integrin $\alpha5$ promotes human mesenchymal stromal cell osteoblast differentiation and osteogenesis. *Proc. Natl. Acad. Sci. U.S.A.* **106,** 18587–18591 CrossRef Medline
48. Damsky, C. H. (1999) Extracellular matrix-integrin interactions in osteoblast function and tissue remodeling. *Bone* **25,** 95–96 CrossRef Medline
49. Burke, P. A., DeNardo, S. J., Miers, L. A., Lamborn, K. R., Matzku, S., and DeNardo, G. L. (2002) Cilengitide targeting of $\alpha_v\beta_3$ integrin receptor synergizes with radioimmunotherapy to increase efficacy and apoptosis in breast cancer xenografts. *Cancer Res.* **62,** 4263–4272 Medline
50. Albert, J. M., Cao, C., Geng, L., Leavitt, L., Hallahan, D. E., and Lu, B. (2006) Integrin $\alpha_v\beta_3$ antagonist Cilengitide enhances efficacy of radiotherapy in endothelial cell and non-small-cell lung cancer models. *Int. J. Radiat. Oncol. Biol. Phys.* **65,** 1536–1543 CrossRef Medline
51. Guan, J.-L. (1997) Role of focal adhesion kinase in integrin signaling. *Int. J. Biochem. Cell Biol.* **29,** 1085–1096 CrossRef Medline
52. Zhou, H., Li, X.-M., Meinkoth, J., and Pittman, R. N. (2000) Akt regulates cell survival and apoptosis at a postmitochondrial level. *J. Cell Biol.* **151,** 483–494 CrossRef Medline
53. Fujita, T., Azuma, Y., Fukuyama, R., Hattori, Y., Yoshida, C., Koida, M., Ogita, K., and Komori, T. (2004) Runx2 induces osteoblast and chondrocyte differentiation and enhances their migration by coupling with PI3K-Akt signaling. *J. Cell Biol.* **166,** 85–95 CrossRef Medline
54. Matzelle, M. M., Gallant, M. A., Condon, K. W., Walsh, N. C., Manning, C. A., Stein, G. S., Lian, J. B., Burr, D. B., and Gravallese, E. M. (2012) Resolution of inflammation induces osteoblast function and regulates the Wnt signaling pathway. *Arthritis Rheum.* **64,** 1540–1550 CrossRef Medline
55. Wu, H., Whitfield, T. W., Gordon, J. A., Dobson, J. R., Tai, P. W., van Wijnen, A. J., Stein, J. L., Stein, G. S., and Lian, J. B. (2014) Genomic occupancy of Runx2 with global expression profiling identifies a novel dimension to control of osteoblastogenesis. *Genome Biol.* **15,** R52 CrossRef Medline
56. Rose-Martel, M., Smiley, S., and Hincke, M. T. (2015) Novel identification of matrix proteins involved in calcitic biomineralization. *J. Proteomics* **116,** 81–96 CrossRef Medline
57. Kassebaum, N. J., Bernabé, E., Dahiya, M., Bhandari, B., Murray, C. J., and Marcenes, W. (2014) Global burden of severe periodontitis in 1990–2010: a systematic review and meta-regression. *J. Dent. Res.* **93,** 1045–1053 CrossRef Medline
58. Beikler, T., and Flemmig, T. F. (2011) Oral biofilm-associated diseases: trends and implications for quality of life, systemic health and expenditures. *Periodontol. 2000* **55,** 87–103 CrossRef Medline
59. Lin, Z., Rios, H. F., and Cochran, D. L. (2015) Emerging regenerative approaches for periodontal reconstruction: a systematic review from the AAP Regeneration Workshop. *J. Periodontol.* **86,** S134–S152 CrossRef Medline

60. Sculean, A., Nikolidakis, D., Nikou, G., Ivanovic, A., Chapple, I. L. C., and Stavropoulos, A. (2015) Biomaterials for promoting periodontal regeneration in human intrabony defects: a systematic review. *Periodontol. 2000* **68,** 182–216 CrossRef Medline
61. Murakami, S. (2017) Emerging regenerative approaches for periodontal regeneration: the future perspective of cytokine therapy and stem cell therapy. in *Interface Oral Health Science 2016*, pp. 135–145, Springer, Singapore
62. Choi, E. Y., Lim, J. H., Neuwirth, A., Economopoulou, M., Chatzigeorgiou, A., Chung, K. J., Bittner, S., Lee, S. H., Langer, H., Samus, M., Kim, H., Cho, G. S., Ziemssen, T., Bdeir, K., Chavakis, E., *et al.* (2015) Developmental endothelial locus-1 is a homeostatic factor in the central nervous system limiting neuroinflammation and demyelination. *Mol. Psychiatry* **20,** 880–888 CrossRef Medline
63. Folwaczny, M., Karnesi, E., Berger, T., and Paschos, E. (2017) Clinical association between chronic periodontitis and the leukocyte extravasation inhibitors developmental endothelial locus-1 and pentraxin-3. *Eur. J. Oral. Sci.* **125,** 258–264 CrossRef Medline
64. Cox, D., Brennan, M., and Moran, N. (2010) Integrins as therapeutic targets: lessons and opportunities. *Nat. Rev. Drug Discov.* **9,** 804–820 CrossRef Medline
65. Wang, H., Yang, H., Shivalila, C. S., Dawlaty, M. M., Cheng, A. W., Zhang, F., and Jaenisch, R. (2013) One-step generation of mice carrying mutations in multiple genes by CRISPR/Cas-mediated genome engineering. *Cell* **153,** 910–918 CrossRef Medline
66. Mashiko, D., Young, S. A., Muto, M., Kato, H., Nozawa, K., Ogawa, M., Noda, T., Kim, Y. J., Satouh, Y., Fujihara, Y., and Ikawa, M. (2014) Feasibility for a large scale mouse mutagenesis by injecting CRISPR/Cas plasmid into zygotes. *Dev. Growth Differ.* **56,** 122–129 CrossRef Medline
67. Henao-Mejia, J., Williams, A., Rongvaux, A., Stein, J., Hughes, C., and Flavell, R. A. (2016) Generation of genetically modified mice using the CRISPR-Cas9 genome-editing system. *Cold Spring Harb. Protoc.* **2016,** pdb.prot090704 CrossRef Medline
68. Ran, F. A., Hsu, P. D., Wright, J., Agarwala, V., Scott, D. A., and Zhang, F. (2013) Genome engineering using the CRISPR-Cas9 system. *Nat. Protoc.* **8,** 2281–2308 CrossRef Medline
69. Cong, L., Ran, F. A., Cox, D., Lin, S., Barretto, R., Habib, N., Hsu, P. D., Wu, X., Jiang, W., Marraffini, L. A., and Zhang, F. (2013) Multiplex genome engineering using CRISPR/Cas systems. *Science* **339,** 819–823 CrossRef Medline
70. Lagares, D., Santos, A., Grasberger, P. E., Liu, F., Probst, C. K., Rahimi, R. A., Sakai, N., Kuehl, T., Ryan, J., Bhola, P., Montero, J., Kapoor, M., Baron, M., Varelas, X., Tschumperlin, D. J., *et al.* (2017) Targeted apoptosis of myofibroblasts with the BH3 mimetic ABT-263 reverses established fibrosis. *Sci. Transl. Med.* **9,** eaal3765 CrossRef Medline
71. Marampon, F., Bossi, G., Ciccarelli, C., Di Rocco, A., Sacchi, A., Pestell, R. G., and Zani, B. M. (2009) MEK/ERK inhibitor U0126 affects *in vitro* and *in vivo* growth of embryonal rhabdomyosarcoma. *Mol. Cancer Ther.* **8,** 543–551 CrossRef Medline
72. Asonova, S. N., and Migalkin, N. S. (1996) [Use of Masson's trichrome method for staining decalcified bone tissue]. *Arkh. Patol.* **58,** 66–67 Medline
73. Tang, X. L., Wang, C. N., Zhu, X. Y., and Ni, X. (2015) Rosiglitazone inhibition of calvaria-derived osteoblast differentiation is through both of PPAR$\gamma$ and GPR40 and GSK3$\beta$-dependent pathway. *Mol. Cell Endocrinol.* **413,** 78–89 CrossRef Medline
74. Kalajzic, I., Kalajzic, Z., Kaliterna, M., Gronowicz, G., Clark, S. H., Lichtler, A. C., and Rowe, D. (2002) Use of type I collagen green fluorescent protein transgenes to identify subpopulations of cells at different stages of the osteoblast lineage. *J. Bone Miner. Res.* **17,** 15–25 CrossRef Medline